

Recognition Ability of Interval Fusion with Preference Aggregation in Weld Defects Images Analysis

Sergey V Muravyov, Ekaterina Y Pogadaeva

*National Research Tomsk Polytechnic University
Pr. Lenina, 30, Tomsk, 634050, Russian Federation, muravyov@tpu.ru*

Abstract – This paper describes a potential applicability of the interval fusion with preference aggregation (IF&PA) approach to the weld image segmentation as the key stage in recognizing a welding joint defective region. In the proposed method, the weld image is divided into a series of equal horizontal bands. For each band, an intensity histogram is plotted, using which the lower and upper bounds are defined for the intervals, which are expected to characterize the defect (foreground) and defect-free (background) areas. The intervals are represented by inrankings forming the foreground and background preference profiles. The Kemeny ranking algorithm is applied to the two profiles in order to determine the best representative points values (in RGB code) of the foreground and background areas. The values serve then as seed parameters of the region growing algorithm applied to distinguish defect and background regions during the segmentation. This approach was tested in segmenting a number of typical weld defect images. The experimental results showed that the proposed approach allows to accurately separate the defect-free region from the defective one.

Keywords – *Weld, Defect, Segmentation, Image processing, Region Growing, Interval Fusion, Preference Aggregation.*

I. INTRODUCTION

Quality control of welding is one of the most important activities of testing, diagnostics and inspection. An integral part of this process is the visual inspection of weld surface, carried out in accordance with ISO 17637: 2016 [1]. The visual control process is very time-consuming and monotonous for the operator, especially under large spatial extent and complex configuration of controlled objects. The inspection process can be automated using image processing methods that typically implement image acquisition, pre-processing, image

segmentation, extraction of defects and their classification [2].

Pre-processing is required to improve image quality. The "raw" image of the weld joint is converted to a uniform appearance, for example, a color image is converted to grayscale, uninformative or less informative areas are removed, etc. If necessary, at this stage, the image is filtered to blur the brightness differences and remove outliers [3].

The key stage in recognizing a defective region is the image segmentation [4,5]. Therefore, the quality of defect recognition depends on the choice of segmentation method and its fine tuning. Currently, known segmentation methods are based on the selection of a region of uniform brightness or color by setting the initial conditions [6,7]. A common disadvantage of these methods is that they are not able to give an integral characteristic of the defective area. Defective areas in the photo image often have a non-uniform brightness, which is associated with differences in the depth of the defect and the quality of lighting when receiving a photo image of the weld. Even after the pre-processing stage that precedes the segmentation, it is not always possible to achieve color uniformity in the defective region. Therefore, it is necessary to merge the segments with different levels of brightness [7].

The aim of this paper is to describe a method of weld image segmentation based on the approach proposed by the authors, interval fusion with preference aggregation (IF&PA), which proved to be reliable and accurate when processing heteroscedastic data [8,9].

II. WELD DEFECTS IMAGES SEGMENTATION

In this paper, image segmentation is of particular interest to us. At this stage of recognition, using the uniformity criterion, the image is divided into two areas: a defect area (foreground) and a defect-free area (background). The defect area is characterized by a significantly darker color than the defect-free area. Moreover, if a defect-free area has dark regions, then it is

likely that they will be recognized as defects, despite the measures taken during preliminary processing.

A. Thresholding

The simplest segmentation method is thresholding, in which the threshold value d is used as a uniformity criterion in the form of an RGB code of a color of the defect area [7]. It is often sufficient to assign a black color code as the threshold d , since a defect in the weld joint will be black after the image is converted to the grayscale. In this case, an automatic segmentation mode is implemented.

If a defect-free area contains dark regions, then for their correct recognition, an interactive mode is required. In the mode, certain pixels are marked on the image (for example, using a "mouse"), the shades of gray of which, according to the operator, characterize the defective area in the best way. The threshold value d in this mode is calculated as some *average* of the colors of the selected pixels (that is, the value of the RGB code), which characterizes the predominant shade of gray for the defect area.

Thresholding was implemented by the authors in the algorithm for computer-aided defect recognition (CADR) in welded joints, implemented in MATLAB and described in [10]. Experimental verification of the algorithm showed that when recognizing a "burn through" defect type (subgroup 105 of the ISO 6520-1: 2007 [11] standard), see Fig. 1, an interactive mode was required. Indeed, in the upper part of the recognized image there are defect-free areas that can be recognized as defects due to the presence of dark regions, and the lower part of the defect image has relatively light regions that can be taken as a defect-free area. To solve the problem, the operator interactively selected pixels with a specific shade of gray in the defective area using the mouse, which made it possible to estimate the binarization threshold d . This led to a more reliable distinction between defect and defect-free areas of the weld. However, note that the lower part of the defect remained unrecognized even in the interactive mode, since its shade of gray was closer to the color of the defect-free area.

To avoid a use of the interactive mode, it is desirable to apply a more advanced segmentation method. One of these methods is Region Growing.

B. Segmentation by Region Growing method

Region Growing – is a group of image segmentation methods based on the use of local image attributes [12,13].

The idea of the method is to analyze first the starting point (seed), then its neighboring points, etc. in accordance with some criterion of homogeneity (for example, pixels in a certain range of grayscale), and in the subsequent enrollment of the analyzed points in one or

another region (the number of starting points should be equal to the number of homogeneous regions in the image). In other versions of the method, the starting point is not individual pixel, but the division of the image into a series of small regions. Then each region is checked for uniformity, and if the test result is negative, then the corresponding area is divided into smaller sections. The process continues until all the selected areas pass the uniformity test. After that, the formation of homogeneous regions begins by means of growing.

Notice that since the regions are grown based on the uniformity criterion, the information about the image, which is contained in its histogram, can be useful. In MATLAB, in Image Segmenter application, it is possible to create a function that implements the method of region growing. We have created such a function, that segments the image C into foreground and background regions, with the following syntax:

$$BW = \text{regionGrowing}(C, f, b), \quad (1)$$

where BW is the image after segmentation, f and b specify the linear indices (seeds) of the pixels in the image marked as foreground and background, respectively.

The accuracy of the initial seed values f and b , which play part of representatives of their regions, definitely impacts the final segmentation result. Therefore, the way in which the appropriate values f and b are selected is very important when applying the method. For example, selection by simple averaging of specified pixels colors is unlikely to be useful, as shown in Section II.A.

In the rest of this article, we intend to show how the IF&PA method can be useful in choosing seed values f and b .

III. INTERVAL FUSION WITH PREFERENCE AGGREGATION METHOD

The IF&PA method begins to work on a set of initial intervals $\{I_k\}$, $k = 1, \dots, m$, describing some data of arbitrary origin such as measurement or computing results. The centers x_k of the intervals are usually known, and their lower and upper bounds are also known or can be formally determined as $x_k \pm u_k$ for given u_k .

The key idea of the method is to transform initial intervals into rankings constructed from discrete values belonging to the intervals, and determine the best discrete value in a consensus ranking as a result. This transformation enables essential information of input interval data to be revealed regardless of data distribution law [8].

The IF&PA method consists of the three main stages presented below.

1. Generating a *range of actual values* (RAV)
 $A = \{a_1, a_2, \dots, a_n\}$:

- find the RAV as a union of initial intervals $\{I_k\}$, $k = 1, \dots, m$, such that the least lower bound and

the largest upper bound among all I_k become the lower and upper bounds of the union correspondently;

- break the RAV into $n - 1$ equal subintervals of length (or *norm*) $h = (a_n - a_1) / (n - 1)$ to obtain the discrete values a_2, a_3, \dots, a_{n-1} ; the number n , or *cardinality* of the RAV partition, can be selected in accordance with recommendations given in [8,9] or taking into account other considerations that are relevant in a particular situation.

2. Representing intervals by rankings λ_k induced by intervals $\{I_k\}$, which we call *inrankings*:

- compose inrankings λ_k using the following conditions for $i, j = 1, \dots, n$:

$$\begin{aligned} a_i \in I_k \wedge a_j \notin I_k &\Rightarrow a_i \succ a_j; \\ a_i, a_j \in I_k \vee a_i, a_j \notin I_k &\Rightarrow a_i \sim a_j; \\ a_i \notin I_k \wedge a_j \in I_k &\Rightarrow a_i \prec a_j; \\ a_i, a_j \in I_k \text{ are neighbors} &\Rightarrow j \equiv i + 1, \end{aligned} \quad (2)$$

where $a_i \succ a_j$ is a strict order relation and $a_i \sim a_j$ is a tolerance relation;

- form the input preference profile $\Lambda = \{\lambda_1, \lambda_2, \dots, \lambda_m\}$ consisting of m inrankings λ_k .

3. Determining a fusion result x^* as the most preferable alternative in consensus ranking β_{fin} for the profile Λ :

- aggregate inrankings Λ by recursive algorithm RECURSALL [14] implementing the *Kemeny rule*, find *all possible consensus rankings* as an output profile $B(N, n) = \{\beta_1, \beta_2, \dots, \beta_N\}$ and transform it into a single *final consensus ranking* β_{fin} by the convolution rule [15]: for all $i < j, i, j = 1, \dots, n$,

$$(r_i < r_j \Rightarrow a_i \succ a_j) \wedge (r_i = r_j \Rightarrow a_i \sim a_j), \quad (3)$$

where relations \succ and \sim are over the single final

consensus ranking β_{fin} , $r_i = \sum_{k=1}^N r_i^k$ is a total rank r_i of the alternative a_i and the rank r_i^k is a position of the alternative a_i in the consensus ranking $\beta_k \in B$.

- assign the most preferable alternative a_i which takes the leftmost position in the obtained ranking β_{fin} to be a fusion result x^* ; if β_{fin} contains more than one best alternatives, then a *sample median* is used as a natural single representative of all these alternatives.

IV. WELD DEFECTS IMAGES SEGMENTATION USING IF&PA

Let us describe the sequence of actions implemented in the language of technical calculations MATLAB, during segmentation by the example of detecting a "burn-through" defect on a photographic image of a weld (see Fig. 1).

Let the initial color image of the welded joint (Fig. 1a) be represented by the $(n \times m)$ matrix $A = [a_{ij}]$ of pixels in RGB format, consisting of $i = 1, \dots, n$ rows and $j = 1, \dots, m$ columns.

Let the initial color image of the welded joint (Fig. 1a) be represented by the $(n \times m)$ matrix $A = [a_{ij}]$ of pixels in RGB format, consisting of $i = 1, \dots, n$ rows and $j = 1, \dots, m$ columns.

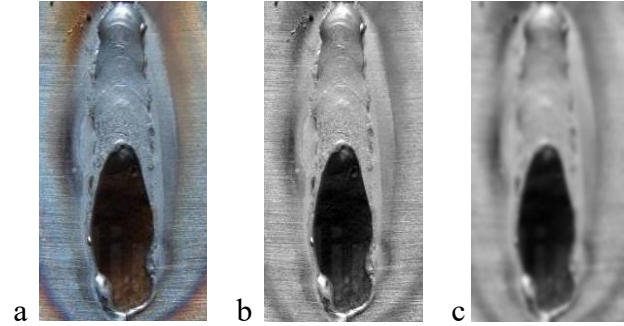


Fig. 1. Image pre-processing of a "burn-through" defect: a) initial image A, b) grayscale image B, c) image after filtration C

1. Using the *rgb2gray* function, a color image A is converted into a grayscale image $B = [b_{ij}]$, consisting of 256 shades of gray (Fig. 1b).

2. To suppress luminance interference, the grayscale image B is converted to $C = [c_{ij}]$ (Fig. 1c) using a Gaussian filter (*imgaussfilt* function).

3. Using the *imcrop* function, the image C is divided into 10 horizontal subregions (bands) C_1, \dots, C_{10} of equal width (Fig. 2). Note that the selection of the appropriate number of bands is a subject for a separate study. In present work, we consider this number to be given.

4. The construction of intensity histograms for each band C_1, \dots, C_{10} is performed using the *imhist* (C) function (Fig. 2). A grayscale histogram is a graphical discrete function that describes the frequency at which the gray level appears in an image. The abscissa of the graph shows the RGB codes of gray levels (intensity or brightness), and the ordinate shows the number of pixels for a given gray level.

5. For each band $C_k, k = 1, \dots, 10$, the bounds of the interval $F_k = [f_k^l, f_k^u]$ corresponding to the range of gray levels of the *image foreground* (dark, i.e. defective, area) are determined:

- the lower bound f_k^l of the interval is equal to the RGB-code value of the darkest pixel on the histogram;
- the upper bound f_k^u of the interval is equal to the *average value* of the histogram.

Boundary values of the *image foreground* intervals F_k for the set of bands shown in Fig. 2 are given in Table. 1.

6. The obtained set of intervals $F_k, k = 1, \dots, 10$, is fed to the input of the IF&PA procedure (see Section III),

which forms the RAV, as shown in Fig. 3. The number of subintervals $n - 1$ of the partition is chosen equal to 10. Lower and upper RAV's bounds are equal to 0 and 115 respectively, therefore, the norm $h = 115 / 10 = 11.5$. The obtained discrete values a_1, a_2, \dots, a_{11} are shown in Fig. 3. The preference profile constructed for intervals F_k is as follows:

$\lambda_1: a_2 \sim a_3 \sim a_4 \sim a_5 \sim a_6 \succ a_1 \sim a_7 \sim a_8 \sim a_9 \sim a_{10} \sim a_{11}$
 $\lambda_2: a_5 \sim a_6 \sim a_7 \succ a_1 \sim a_2 \sim a_3 \sim a_4 \sim a_8 \sim a_9 \sim a_{10} \sim a_{11}$
 $\lambda_3: a_6 \sim a_7 \sim a_8 \sim a_9 \sim a_{10} \sim a_{11} \succ a_1 \sim a_2 \sim a_3 \sim a_4 \sim a_5$
 $\lambda_4: a_6 \sim a_7 \sim a_8 \sim a_9 \succ a_1 \sim a_2 \sim a_3 \sim a_4 \sim a_5 \sim a_{10} \sim a_{11}$
 $\lambda_5: a_1 \sim a_2 \succ a_3 \sim a_4 \sim a_5 \sim a_6 \sim a_7 \sim a_8 \sim a_9 \sim a_{10} \sim a_{11}$
 $\lambda_6: a_1 \succ a_2 \sim a_3 \sim a_4 \sim a_5 \sim a_6 \sim a_7 \sim a_8 \sim a_9 \sim a_{10} \sim a_{11}$
 $\lambda_7: a_1 \succ a_2 \sim a_3 \sim a_4 \sim a_5 \sim a_6 \sim a_7 \sim a_8 \sim a_9 \sim a_{10} \sim a_{11}$
 $\lambda_8: a_1 \succ a_2 \sim a_3 \sim a_4 \sim a_5 \sim a_6 \sim a_7 \sim a_8 \sim a_9 \sim a_{10} \sim a_{11}$
 $\lambda_9: a_2 \sim a_3 \succ a_1 \sim a_4 \sim a_5 \sim a_6 \sim a_7 \sim a_8 \sim a_9 \sim a_{10} \sim a_{11}$
 $\lambda_{10}: a_2 \sim a_3 \sim a_4 \sim a_5 \sim a_6 \succ a_1 \sim a_7 \sim a_8 \sim a_9 \sim a_{10} \sim a_{11}$

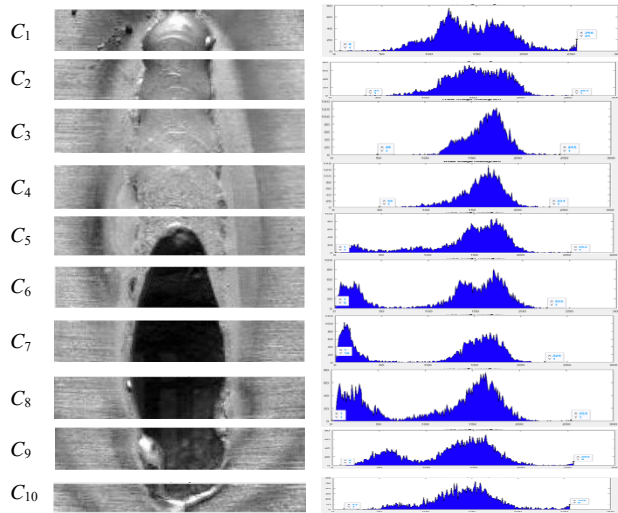


Fig. 2. Image C partition into 10 horizontal bands C_1, \dots, C_{10} of equal width, on the left are the band histograms

Table 1. Boundary values of the image foreground intervals F_k for the set of bands shown in Fig. 2.

Band	Lower bound	Upper bound
C_1	5	65
C_2	38	80
C_3	49	115
C_4	50	95
C_5	0	10
C_6	0	5
C_7	0	5
C_8	0	5
C_9	10	30
C_{10}	12	55

At the IF&PA output, after convolution (3), we get the final consensus ranking:

$\beta_{\text{fin}}: a_6 \succ a_2 \sim a_1 \succ a_5 \sim a_3 \sim a_7 \succ a_4 \sim a_8 \sim a_9 \succ a_{10} \succ a_{11},$

whence we have $x^* = a_6 = 57.5 \approx 58$, which we take as the value of the foreground grayscale level, i.e. $f = 58$.

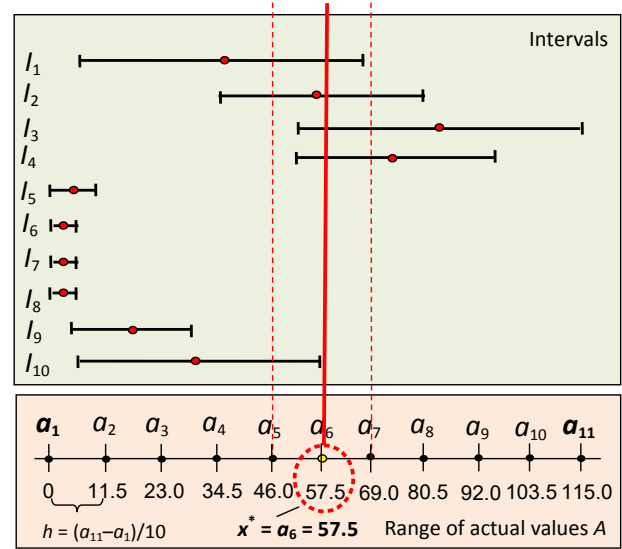


Fig. 3. Example of how the IF&PA method works where are shown: initial collection of $m = 10$ intervals $\{F_k\}$, $k = 1, \dots, 10$; range of actual values $A = \{a_1, \dots, a_{11}\}$; its partition into $n = 10$ meshes; the interval fusion result $x^* = 57.5$

7. For each band C_k , $k = 1, \dots, 10$, the middle point and the bounds of the interval $B_k = [b_k^l, b_k^u]$ corresponding to the range of gray levels of the image background (light, i.e. defect-free, area) are determined:

- the middle point b_k^c of the interval is equal to the RGB-code corresponding to the maximum bin height in the histogram;
- the lower bound $b_k^l = 0.9b_k^c$,
- the upper bound $b_k^u = 1.1b_k^c$.

Boundary values of the image background intervals B_k for the set of bands shown in Fig. 2 are given in Table 2.

Table 2. Boundary values of the image background intervals B_k for the set of bands shown in Fig. 2.

Band	Lower bound	Upper bound
C_1	100	120
C_2	140	180
C_3	160	180
C_4	170	180
C_5	160	170
C_6	130	150
C_7	140	180
C_8	140	160
C_9	140	160
C_{10}	160	170

8. The obtained set of intervals B_k , $k = 1, \dots, 10$, is fed to the input of the IF&PA procedure, which again forms the RAV. As before, the number of subintervals $n - 1$ of the partition equals to 10. Lower and upper RAV's bounds are equal to 100 and 180 respectively, therefore, the norm $h = 180 - 100 / 10 = 8$. The obtained discrete values a_1, a_2, \dots, a_{11} are correspondingly 100, 108, ..., 180. The preference profile constructed for intervals B_k is as follows:

$$\begin{aligned} \lambda_1: a_1 \sim a_2 \sim a_3 > a_4 \sim a_5 \sim a_6 \sim a_7 \sim a_8 \sim a_9 \sim a_{10} \sim a_{11} \\ \lambda_2: a_6 \sim a_7 \sim a_8 \sim a_9 \sim a_{10} \sim a_{11} > a_5 \sim a_4 \sim a_3 \sim a_2 \sim a_1 \\ \lambda_3: a_9 \sim a_{10} \sim a_{11} > a_1 \sim a_2 \sim a_3 \sim a_4 \sim a_5 \sim a_6 \sim a_7 \sim a_8 \\ \lambda_4: a_{10} \sim a_{11} > a_1 \sim a_2 \sim a_3 \sim a_4 \sim a_5 \sim a_6 \sim a_7 \sim a_8 \sim a_9 \\ \lambda_5: a_9 > a_1 \sim a_2 \sim a_3 \sim a_4 \sim a_5 \sim a_6 \sim a_7 \sim a_8 \sim a_{10} \sim a_{11} \\ \lambda_6: a_5 \sim a_6 \sim a_7 \sim a_8 > a_1 \sim a_2 \sim a_3 \sim a_4 \sim a_9 \sim a_{10} \sim a_{11} \\ \lambda_7: a_6 \sim a_7 \sim a_8 \sim a_9 \sim a_{10} \sim a_{11} > a_1 \sim a_2 \sim a_3 \sim a_4 \sim a_5 \\ \lambda_8: a_6 \sim a_7 \sim a_8 > a_1 \sim a_2 \sim a_3 \sim a_4 \sim a_5 \sim a_9 \sim a_{10} \sim a_{11} \\ \lambda_9: a_6 \sim a_7 \sim a_8 > a_1 \sim a_2 \sim a_3 \sim a_4 \sim a_5 \sim a_9 \sim a_{10} \sim a_{11} \\ \lambda_{10}: a_9 > a_1 \sim a_2 \sim a_3 \sim a_4 \sim a_5 \sim a_6 \sim a_7 \sim a_8 \sim a_{10} \sim a_{11} \end{aligned}$$

At the IF&PA output, after convolution (3), we get the final consensus ranking:

$$\beta_{\text{fin}}: a_6 \sim a_9 > a_7 \sim a_{10} \sim a_{11} > a_8 \sim a_2 > a_1 \sim a_3 > a_4 \sim a_5,$$

whence we have $x^* = (a_6 + a_9) / 2 = (140 + 169) / 2 = 154.5 \approx 155$, which we take as the value of the background grayscale level, i.e. $b = 155$.

9. Finally, we run the *regionGrowing* (C, f, b) function (see Section II.B), where f and b values obtained in steps 6 and 8 respectively are used as initial conditions and the function parameters.

V. RESULTS AND DISCUSSIONS

Fig. 4 shows the results of segmentation by the method of region growing without and with the use of IF&PA by the example of "burn through" defect image. It is clear from Fig. 4 that arbitrary assignment of starting points leads to an insufficiently correct segmentation result in the form of two excess light regions and one excess dark region, while the use of the IF&PA made it possible to very accurately identify the defect area in the image.

Fig. 5 and Fig. 6 show the results of a similar analysis of images of other types of defects such as "crack" and "multiple defect". As one can see, in these cases the IF&PA use again provides high segmentation accuracy.

VI. CONCLUSIONS AND OUTLOOK

It is shown in the paper how one can improve the quality of segmentation in the process of recognizing weld defects in photographic images. Such a segmentation method as region growing is quite effective.

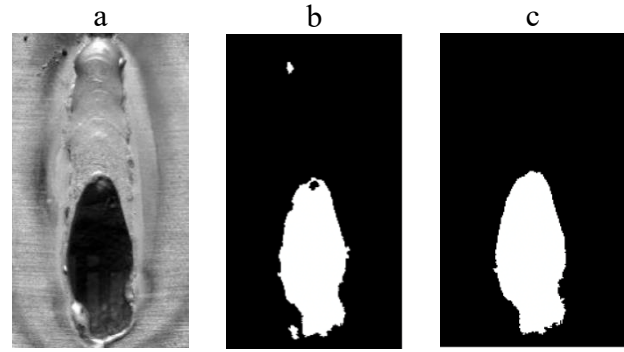


Fig. 4. Segmentation of a "burn-through" image: a) original image, b) region growing result, c) region growing in combination with IF&PA result

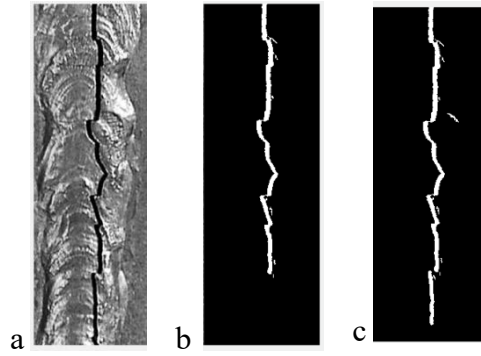


Fig. 5. Segmentation of a "longitudinal crack" image: a) original image, b) region growing result, c) region growing in combination with IF&PA result

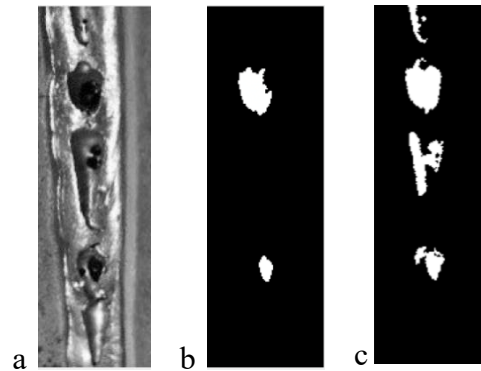


Fig. 6. Segmentation of a "multiple defect" image: a) original image, b) region growing result, c) region growing in combination with IF&PA result

However, for its correct application, the selection of appropriate starting point values is required. It is proposed to use the IF&PA method for this purpose. A special procedure has been developed for the combined application of methods of region growing and the IF&PA. Based on specific examples of recognizing weld defects of various types, it is shown that the IF&PA

improves the accuracy of segmentation stage and, consequently, of recognition in general.

In the course of further research, it is planned to carry out a statistical analysis of the application of IF&PA for segmentation with a different number of the image C partitions into bands. We also going to develop a formal justification for calculating the boundaries of the intervals F_k and B_k based on the information contained in the histograms of the corresponding bands.

VII. ACKNOWLEDGMENTS

This work was supported by the Russian Science Foundation, project # 18-19-00203.

REFERENCES

- [1] **ISO 17637:2016**: Non-destructive testing of welds – Visual testing of fusion-welded joints.
- [2] **Dong, S., Sun, X., Xie, S., Wang, M.**: Automatic defect identification technology of digital image of pipeline weld, *Natural Gas Industry B*, Vol. 6, No. 4, 2019, pp. 399–403.
- [3] **Saranya, R., Daniel, J., Abudhahir, A., Chermakani, N.**: Comparison of segmentation techniques for detection of defects in non-destructive testing images, *In 2014 International Conference on Electronics and Communication Systems (ICECS)*, 2014, pp. 1–6.
- [4] **Al-Hameed, W.**: Segmentation of radiographic images of weld defect, *Journal of Global Research in Computer Science*, Vol. 4, No. 7, 2013, pp. 1–4.
- [5] **Mahmoudi, A., Regragui, F.**: Welding defect detection by segmentation of radiographic images, *In 2009 WRI World Congress on Computer Science and Information Engineering IEEE*, Vol. 7, 2009, pp. 111–115.
- [6] **Hore S., Chakraborty S., Chatterjee, S., et al.**: An integrated interactive technique for image segmentation using stack based seeded region growing and thresholding, *International Journal of Electrical & Computer Engineering*, Vol. 6, No. 6, 2016, pp. 2088–8708.
- [7] **Umbugh, S.E.**: *Digital Image Processing and Analysis. Applications with MATLAB and CVPtools*, CRC Press, Boca Raton, 2017.
- [8] **Muravyov, S.V.; Khudonogova, L.I.; Emelyanova, E.Y.**: Interval data fusion with preference aggregation, *Measurement*, Vol. 116, 2018, pp. 621–630.
- [9] **Muravyov, S.V., Khudonogova, L.I., Ho, M.D.**: Adjustment of fundamental physical constant values using the interval fusion with preference aggregation, *Measurement*, Vol. 163, 2020, 108037.
- [10] **Muravyov, S.V.; Pogadaeva, E.Yu.**: Computer-aided recognition of defects in welded joints during visual inspections based on geometric attributes, *Russian Journal of Nondestructive Testing*, Vol. 56, No. 3, 2020, pp. 259–267.
- [11] **ISO 6520-1:2007** *Welding and allied process – Classification of geometric imperfections in metallic materials*, Part 1: Fusion welding.
- [12] **Preetha, M.M.S.J., Suresh, L.P., Bosco, M.J.**: Image segmentation using seeded region growing, *International Conference on Computing, Electronics and Electrical Technologies (ICCEET)*, 2012, pp. 576–583.
- [13] **Gómez, O., González, J.A., Morales, E.F., Rueda, L., Mery, D., Kittler, J.**: Image segmentation using automatic seeded region growing and instance-based learning, *Progress in Pattern Recognition, Image Analysis and Applications*, 192–201, Springer Berlin Heidelberg, 2007.
- [14] **Muravyov, S.V.**: Ordinal measurement, preference aggregation and interlaboratory comparisons, *Measurement*, Vol. 46, No. 8, pp. 2927–2935.
- [15] **Muravyov, S.V., Baranov, P.F., Emelyanova, E.Y.**: How to transform all multiple solutions of the Kemeny Ranking Problem into a single solution, *Journal of Physics: Conference Series*, Vol. 1379, 2019, 012053.